Shell transitions between metastable states of Yukawa balls

S. Käding,[1] D. Block,[2] A. Melzer,[1] A. Piel,[2] H. Kählert,[3] P. Ludwig,[3] and M. Bonitz[3]
[1]*Institut für Physik, Ernst-Moritz-Arndt-Universität, D-17487 Greifswald, Germany*
[2]*IEAP, Christian-Albrechts-Universität, D-24098 Kiel, Germany*
[3]*ITAP, Christian-Albrechts-Universität, D-24098 Kiel, Germany*

(Received 3 June 2008; accepted 30 June 2008; published online 31 July 2008)

Spherical dust clusters composed of several concentric shells are experimentally investigated with particular interest on transitions between different configurations and transitions of particles between different shells. Transitions between different ground and metastable configurations are frequently observed. The experimental analysis allows us to derive the energy differences of different configurations from particles traveling between shells. The observed transitions and transition probabilities are compared to molecular dynamics simulations. © *2008 American Institute of Physics*. [DOI: 10.1063/1.2961080]

I. INTRODUCTION

Coulomb crystallization processes have been studied by means of electrons on helium,[1] metallic particles in Paul traps[2] or laser-cooled trapped ions[3,4] where the regime of strong coupling is achieved at very low kinetic energies.[5] Alternatively, complex or dusty plasmas can be used to study strong coupling effects. Dusty plasmas are ionized gases containing highly charged nanometer to micrometer sized particles. The particles are charged by the continuous inflow of electrons and ions to the particle. Depending on plasma and particle conditions fluidlike behavior as well as crystallization can be realized even at room temperature. A particularly interesting example of complex plasmas are Yukawa balls[6] where tens to thousands of highly charged microparticles arrange on spherical, nested shells. The clouds which are confined in a radio frequency discharge are highly transparent and allow direct observation with video cameras and to study the dynamics on the level of individual particles.

From previous experiments[6,7] and simulations[8–15] it is known that finite systems of charged particles trapped in a spherical confinement arrange in nested spherical shells with occupation numbers $(N_1, N_2, \ldots)$, where N_j is the number of particles on the jth shell (starting with the innermost shell). On each shell the particles arrange in a hexagonal lattice (with only a few dislocations)[12] as shown in experiments on laser-cooled ions[3,4] and on Yukawa balls.[6] Yukawa balls in dusty plasmas differ from ion clusters by a shielded interaction due to screening of the dust particles by the surrounding plasma. While the pure Coulomb interaction in ion clusters leads to a strictly homogeneous particle density, a radial density gradient is found for the shielded interaction in Yukawa balls.[16]

The structure and formation of ground and metastable states of Yukawa balls has been studied recently.[16] The analysis of these states plays an important role in the understanding of melting transitions of finite clusters. The melting transitions of clusters with magic configurations has theoretically been investigated for Coulomb and screened interactions.[17] Here we present new experimental observations of clusters with different particle numbers ranging from $N=17$ to $N=91$, where changes of the shell population due to transitions of particles between cluster shells have been studied. In this paper we concentrate on the discussion of shell transitions. However, the analysis of the shell transitions requires a knowledge of the cluster structure and their metastable states. Thus, both the structure and probability of metastable states and their shell transitions will be described. In addition, molecular dynamics (MD) simulations have been conducted to support and clarify the experimental findings.

The paper is organized as follows: In Sec. II the experimental approach, the camera setup, and the algorithm for three-dimensional particle positioning and tracking is described. Furthermore, the model used for the MD simulations is briefly introduced. In Sec. III the experimental generation of different metastable states is described together with the analysis of the observed clusters. The main part of this paper deals with self-excited transitions of particles between shells. In Sec. IV the shell transitions are studied in the context of the energy difference between different configurations. The findings are discussed in Sec. V. Finally, the results are summarized.

II. EXPERIMENT AND SIMULATION TECHNIQUE

A. Discharge

The experiments have been conducted in a capacitively coupled asymmetric radio frequency discharge at 13.56 MHz in argon at a gas pressure of 90 Pa and a discharge power between 2 and 7.5 W. For trapping of the particles in Yukawa balls we follow the technique of Arp *et al.*[6] Monodisperse plastic spheres of 3.46 μm diameter (mass $m=3.28\times10^{-14}$ kg) are confined horizontally by a cubic glass box placed on the lower electrode. Vertically, gravity is compensated by the combined action of an upward thermophoretic force due to heating of the lower electrode and a weak electric field. Due to the large inertia the relevant dynamical frequencies are of the order of 10 Hz which ensures that the particles are not affected by the applied radio frequency fields.[18] In this trap, which is described in detail in Ref. 19, Yukawa balls are produced where the particles arrange in a spherical cloud with nested concentric shells.

B. Stereoscopic setup

The investigation of structural and dynamical properties of 3D particle systems requires the simultaneous measurement of all particle coordinates. In the literature, different approaches in dusty plasmas have been presented, ranging from the color-gradient method[20] via digital inline holography[21] to stereoscopic methods.[22,23]

For the experiments described here, an improved three-camera stereoscopic setup has been developed. The cameras are oriented pairwise perpendicular to each other to keep the observation geometry as simple as possible. At the same time, the spatial resolution in three dimensions is assured to be equal. In principle, the information collected by two cameras that observe the dust cloud from different directions is sufficient to reconstruct the 3D positions. However, a third camera reduces the problem of overlapping particle images that often leads to ambiguities if only two cameras are used.

The cameras used are high-speed CMOS cameras (Mikrotron 1310) with a spatial resolution of 1280×1024 pixel and a maximum frame rate of 500 frames per second (fps). The three high-speed video cameras are synchronized by an external trigger signal and are operated with up to 25 fps in our experiments. Each of the cameras has its own frame-grabber interface with built-in memory in a separate computer. At low frame rates (<100 fps) the camera data can be saved directly to hard-disk enabling long-running observations of Yukawa balls of a few hours.

The volume observed by the cameras is limited by the focal depth of $10 \times 10 \times 10$ mm^3. An expanded laser beam is necessary to illuminate all the particles in this volume. For this purpose a 600 mW Nd:YAG laser at 532 nm has been chosen so that it matches the maximum spectral sensitivity of the cameras very well. The dust cloud is illuminated from two directions. The horizontal cameras observe the particles in forward scattered light, which offers a higher light intensity, and, in turn, an increased focal depth due to smaller camera apertures.

With this setup the 3D positions of all particles in a Yukawa ball can be measured simultaneously with high spatial and temporal resolution.[24] Thus, the stereoscopic setup allows long-running observations of Yukawa balls to identify spontaneous transitions between configurations. A scheme of the vessel and the stereoscopic high-speed camera setup is shown in Fig. 1.

C. Data analysis

To recover the static and dynamical properties of Yukawa balls, the 3D positions of all particles have to be accurately determined. The processing from sequences of corresponding 2D image triples to the full 3D particle trajectories is performed in several steps.

In the first step, the 2D image coordinates of all particles are determined from the two-dimensional images using standard particle identification techniques, see, e.g., Refs. 25 and 26. This identification is performed for each frame of the three cameras separately. Due to the large amount of video data this step is most time-consuming. Typical video images are shown in Fig. 2.

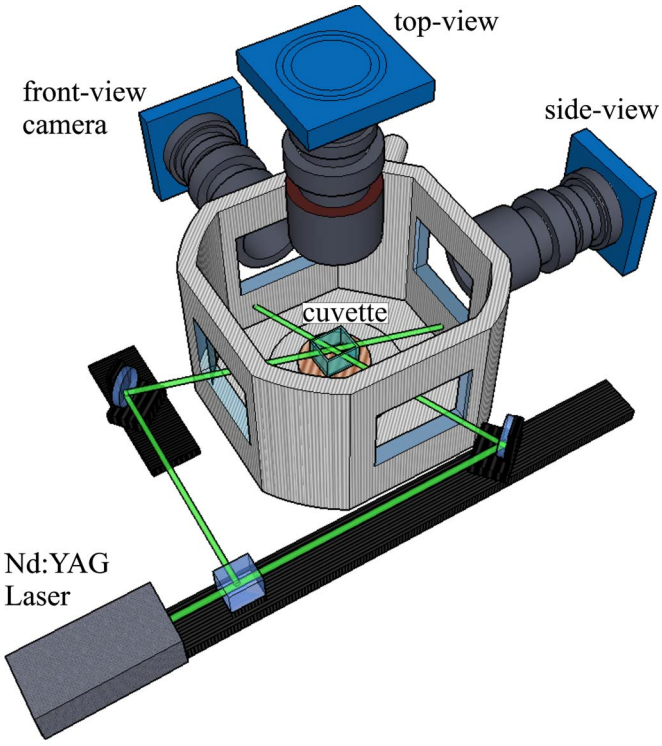

FIG. 1. (Color online) Scheme of the stereoscopic camera setup and illumination. Three pairwise perpendicular oriented high-speed video cameras observe the Yukawa ball inside the glass cuvette. The dust particles are illuminated by an expanded circular laser beam from two directions. The observation of the particles in forward scattered light by the horizontal cameras ensures a higher focal depth.

To reconstruct the 3D particle positions and trajectories, respectively, we rely on the perpendicular optical axes and neglect any distortion due to the imperfections of the camera lenses and windows of the vacuum vessel. In the next step the 2D images of the dust cloud are scaled to the same size and adjusted to their respective center of mass. The search for corresponding particles is performed according to Fig. 3. We exploit here that due to the orthogonal projections each pair of cameras shares a common coordinate. The front-view camera yields the coordinates (Y,Z), the sideview (X,Z), and the top-view camera (X,Y), respectively. Corresponding particles are searched within a small stripe of the common coordinates. The algorithm delivers the 3D trajectories of all particles with only a very few missing samples.

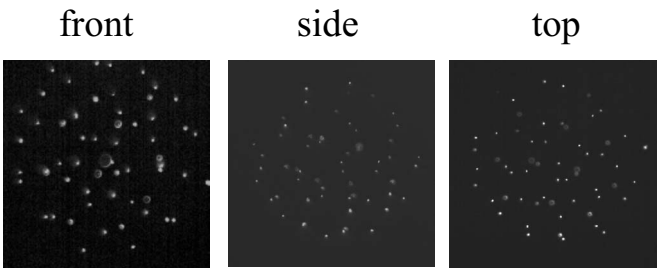

FIG. 2. Raw video still images of a cluster with $N=91$ recorded by the three cameras. The main advantage is that all particles are seen in at least two cameras.

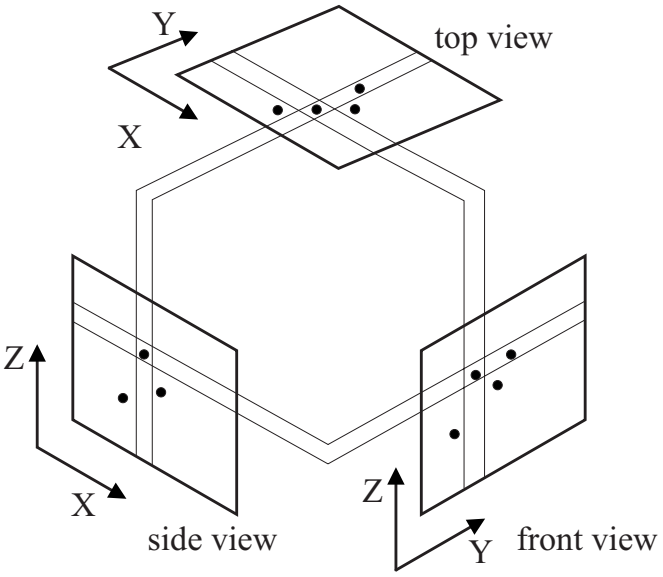

FIG. 3. The search for orthogonal particles projections in corresponding image pairs is delimited to a small range of the common coordinate. With the three-camera setup no uncorrectable shadowing of particles occurs.

D. MD simulations

To analyze the experimentally observed structures of Yukawa balls and to quantify the energies needed for a shell transition, we have performed molecular dynamics (MD) simulations. The structure is found from minimizing the total energy of a system with N particles of charge Z,

$$E = \sum_{i=1}^{N} \frac{p_i^2}{2m} + \sum_{i=1}^{N} \frac{\alpha r_i^2}{2} + \frac{Z^2 e^2}{4\pi\epsilon_0} \sum_{i>j}^{N} \frac{\exp(-r_{ij}/\lambda_D)}{r_{ij}}. \quad (1)$$

Here, α is the strength of the confinement potential for the dust. Further, $r_i = |\vec{r}_i|$ is the radial position of the ith particle and $r_{ij} = |\vec{r}_i - \vec{r}_j|$ is the distance between particles i and j. The first term on the RHS is the kinetic energy of the particles. The second term describes the potential energy of the confinement which is modeled to be isotropic as suggested by the experiments. The third term is the mutual electrostatic energy due to the Yukawa interaction. In simulations, the shielding strength is often defined as $\kappa' = r_0/\lambda_D$, where $r_0^3 = 2Z^2e^2/(4\pi\epsilon_0 m\omega_0^2)$ is a normalized distance. To ease the comparison with the experiment in the simulations the shielding length λ_D is prescribed for every run. Then, the equilibrium interparticle distance is determined in the simulation and the shielding strength $\kappa = b/\lambda_D$ is obtained as the ratio of the interparticle distance b and shielding length λ_D. For our conditions $\kappa \approx 1.3 \ldots 1.5\kappa'$.

The crystalline state of the cluster at room temperature ($T = 300$ K) which corresponds to a thermal energy of 25 meV requires a charge of $Z = 2000$ in the simulation, which is in agreement with previous investigations.[10,19] The parameter α is basically deduced from measurements at similar, but not identical conditions.[19] Hence we allow for slight adjustments to achieve exactly the same cluster dimensions in simulation and experiment. The ground state configuration of a cluster is found from the minimum of E. It is, however, well known that for many particle numbers, metastable configurations exist with only marginally higher energy, see, e.g., Refs. 12 and 27. Equation (1) shows that the ground state configuration of a cluster of N particles depends on the shielding strength κ. For different particle numbers the lowest energy configuration as well as the most probable occurring configuration can be determined for different screening strengths by a systematic variation of κ. For every set of parameters N and κ, a set of 500 runs from random initial particle positions have been performed. Our findings have been validated against the simulations of Refs. 10 and 28, which have been performed for slightly different parameters but with better statistics.

III. FORMATION OF METASTABLE STATES OF YUKAWA BALLS

In the following experiments the formation of metastable states of Yukawa balls is discussed. Since the shape of the cluster and its trapping position sensitively depend on the trap parameters, the cluster structure can be easily destroyed and afterwards re-established by controlled changes of the plasma parameters. During a brief and well-defined interruption of the discharge power the particles start to fall downwards. Before the particles reach the lower electrode, the discharge is reset, the confinement is restored, and the Yukawa ball is newly formed with exactly the same particles.

However, during the particle motion towards the electrode and back into the trapping region the initial crystalline particle arrangement is destroyed. The cluster has lost any memory on its previous arrangement. After the trap is reestablished the particles are allowed to relax into their new equilibrium positions for about 60 s. Afterwards the particle configuration is recorded for 30 s. This procedure can be repeatedly applied to obtain independent realizations of a cluster under identical conditions.

To cover the full range of particle numbers $N < 100$, we show detailed experiments for clusters with $N = 17$, 27, 31, 52, and 91 particles ranging from one shell to three shells. We start with a brief compilation of the observed cluster structures before transitions between different shell configurations and appearance probabilities of metastable states are analyzed.

Snapshots of observed configurations of Yukawa balls for different particle number are shown in Fig. 4. All clusters consist of concentric nested onionlike shells with or without an additional center particle. This is a typical structure of a finite strongly coupled system. Now, we will investigate the structure of these systems and compare the results with simulations.

A. Cluster 1: $N = 17$

The smallest cluster investigated here has $N = 17$ particles. The loss and recovery of the confinement has been repeated 30 times. The experimentally observed configuration always is (1,16). In all 30 repetitions, only this configuration has been found. Simulations[12,27] have identified this configuration to be the ground state for Coulomb interaction. Also for the experimentally relevant values of the screening strength $\kappa < 4.5$, no other ground state configuration as

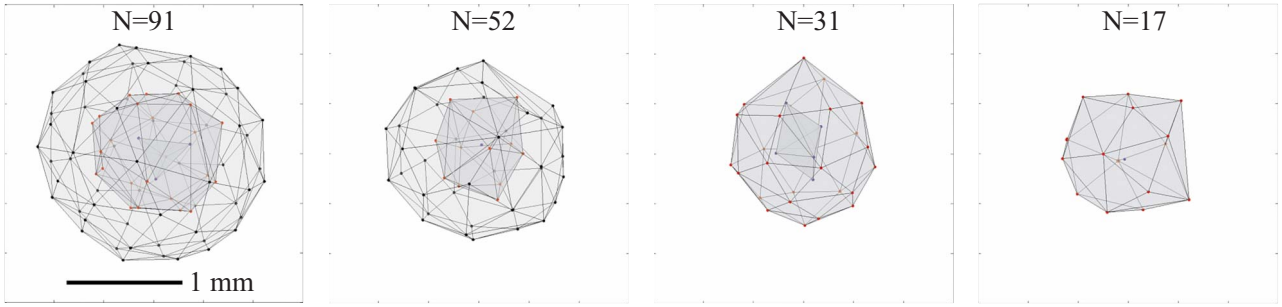

FIG. 4. (Color online) Cluster configurations reconstructed from single video snapshots with $N=91$, 52, 31, and 17. The Yukawa balls consist of concentric shells with the configurations (4,25,62) for the $N=91$, (11,41) for the $N=52$, (5,26) for the $N=31$, and (1,16) for the $N=17$ cluster.

(1,16) exists. For pure Coulomb interaction the configuration (0,17) is an excited state, which has not been observed in the repeated experiments. For the cluster with $N=17$ we have not observed any metastable configuration. This observation has two possible explanations: either a metastable state does not exist, or it is energetically not accessible. More insight is gained when looking at the dynamics in Sec. IV.

B. Cluster 2: *N*=27

Next, a slightly larger cluster $N=27$ is investigated which consists of two shells. Using the repeated formation of Yukawa balls we were able to produce three different configurations, namely (2,25), (3,24), and (4,23) under identical plasma conditions. The different configurations are shown in Fig. 5.

From simulations[29] the ground state configuration is (3,24) for $\kappa<1.5$. For values of the screening strength $\kappa>1.5$ the configuration (4,23) is energetically preferred. The observed state (2,25) is not a ground state configuration. Consequently, this configuration is identified as a metastable state.

It is now very intriguing to address the question, which configuration possesses the *highest probability* of occurrence instead of asking, which has the *lowest energy*. In the repetition experiments, the configuration (3,24) showed the highest probability of 50% (6 out of 12 configurations were observed in this configuration) followed by the configuration (4,23) with 42% (5 out of 12). The configuration (2,25) was observed only once (probability of 8%).

To clarify these experimental observations, we have also performed MD simulations of the $N=27$ cluster. Here a curvature parameter of $\alpha=3.61\times10^{-11}$ kg s^{-2} was used to match the experimental size of the cluster. The kinetic temperature of the particle has been taken in the simulation as $T=300$ K.

Varying the screening strength κ in the simulation, we can study the influence of screening on the appearance probability of the different configurations. The probability of finding a certain metastable configuration in the simulation is shown in Fig. 6. The simulation starts from random particle positions to mimic the experimental loss and recovery of the confinement. It was found that three configurations have a nonvanishing probability for values of κ between 0 and 1.5. The first (2,25) is a metastable configuration and appears only for small κ values. The probability of finding the second configuration (3,24) slowly drops with increased screening strength, whereas a dramatic increase of appearance probability is observed for the third configuration (4,27). Generally speaking, with increasing screening the average occupation number of the inner shell increases. A quantitative agreement of the occurrence in experiment and simulation is found for a screening strength $\kappa=0.8\pm0.2$ which is in agreement with the screening strength derived from structural investigations.[10]

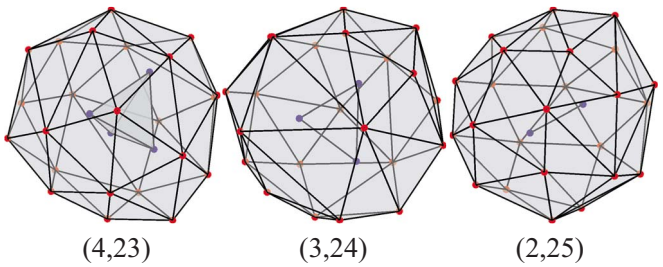

FIG. 5. (Color online) The three experimentally observed configurations of the $N=27$ Yukawa ball.

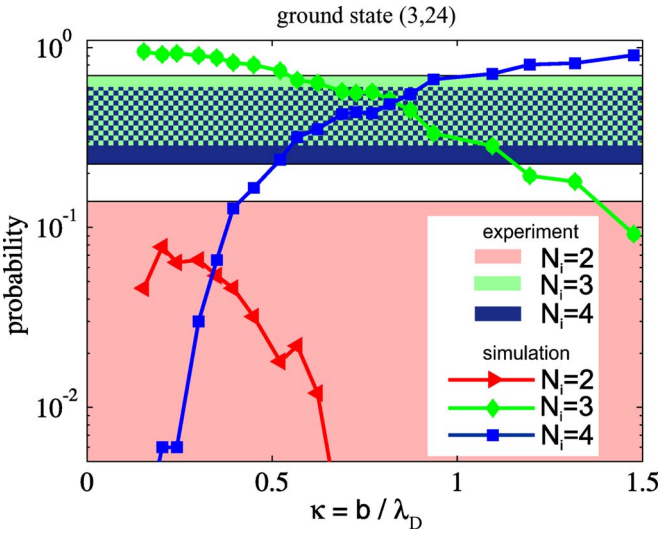

FIG. 6. (Color online) Simulated probability of different metastable states with $N_i=2,3,4$ for a cluster with $N=27$ as a function of screening strength κ. The experimentally observed probabilities are indicated by horizontal stripes and their width describes the uncertainty from counting statistics.

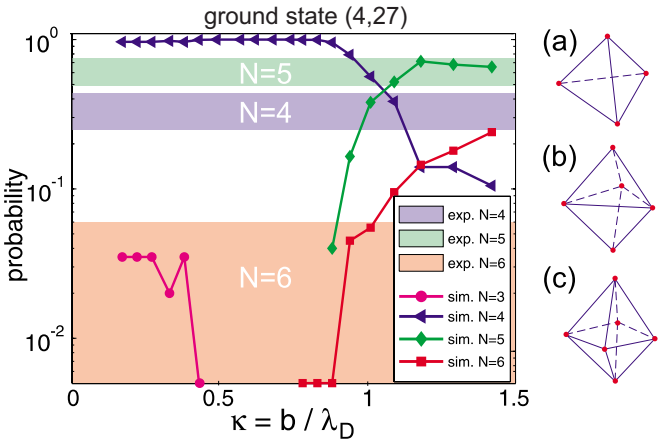

FIG. 7. (Color online) Simulated probability of different metastable states with $N_1=4,5,6$ for a cluster with $N=31$ as a function of screening strength κ. The experimentally observed probabilities are indicated by horizontal stripes. (a), (b), (c) Structure of the inner shell for $N_1=4,5,6$ (Ref. 16).

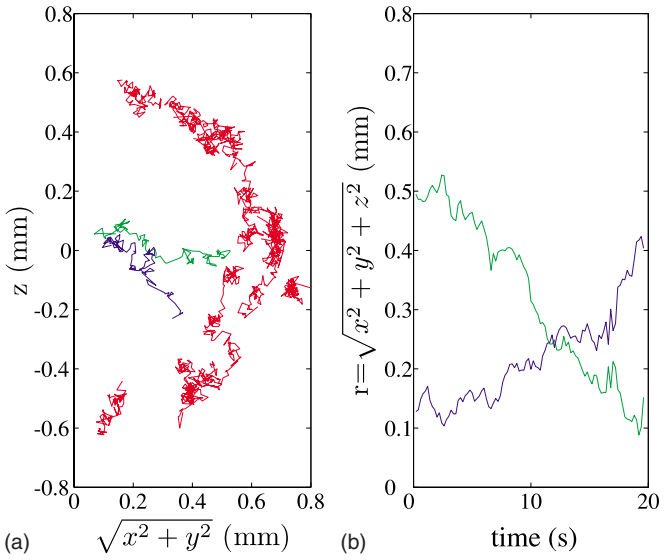

FIG. 8. (Color online) (a) Self-excited transitions of particles in a Yukawa ball with $N=17$. Two particles are moving between the outer shell and the cluster center. (b) Radial coordinate of the two traveling particles as a function of time. It is seen that one particle from the outer shell moves inward. At the same time the central particle moves outwards.

It should be noted that the ground state configuration changes close to the range of κ shown here. The ground state is (3,24) for $\kappa<1.5$ and (4,23) for $\kappa>1.5$.

C. Cluster 3: *N*=31

In a similar manner the $N=31$ particle cluster has been analyzed.[16] A number of 37 realizations of the cluster have been generated at exactly the same plasma and confinement conditions. Here, clusters with $N_1=4$, 5, and 6 particles on the inner shell are observed. Hence, well defined crystalline clusters of different (metastable) states (4,27), (5,26), and (6,25) have been produced in the experiment. The probability of appearance is $13/37=35\%$ for (4,27), $23/37=62\%$ for (5,26), and $1/37=3\%$ for (6,25), respectively.

These probabilities are again compared to corresponding MD simulations.[16] A match between the experimentally observed and simulated appearance probabilities is obtained for a screening strength of $\kappa=1.1$ as shown in Fig. 7. The stronger screening (i.e., decreased Debye length λ_D) for $N=31$ compared to the case of $N=27$ is a direct consequence of the higher plasma density at the higher discharge power where the $N=31$ experiments have been performed. These consistent findings validate our conclusions.

In contrast to the $N=27$ cluster, the cluster $N=31$ has only a single ground state configuration in the range $\kappa<2.3$, namely (4,27). For $\kappa>2.4$ the ground state is (6,25), in a tiny range near $\kappa=2.4$ five particles on the inner shell (5,26) represent the ground state. Interestingly, the ground state configuration (4,27) is not the most probable configuration. Instead, the configuration (5,26), which is energetically favored only in a very small range of κ, is found to be most prominent in the repetition experiments.

IV. SHELL TRANSITIONS

Since metastable states are frequently observed, it is tempting to search for transitions between different states. In the subsequent experiments we have analyzed such spontaneous shell transitions. Instead of repeatedly producing clusters with different configurations from discharge interruption, we have recorded the clusters for long times of the order of minutes to detect whether spontaneous changes in the configurations occur.

A. Cluster 1: *N*=17

Although we did not observe a metastable configuration in case of $N=17$ we have been able to observe transitions of particles between shells. Figure 8(a) shows the trajectories over 20 s in a ρ-z plot, i.e., in cylindrical coordinates [here, $\rho=(x^2+y^2)^{1/2}$]. Two particles are seen to be moving between the outer shell and the cluster center. In Fig. 8(b) the radial components $r=(x^2+y^2+z^2)^{1/2}$ of the two traveling particles are presented as a function of time. This shows that one particle from the outer shell moves inwards and simultaneously the previous central particle is displaced and moves outwards. It is important to note that despite of these two transitions the configuration of the cluster remains (1,16) at any time. As soon as one particle enters the inner shell the other particle leaves it. This also indicates that the configuration (2,15) is not stable under our conditions. A detailed analysis of the particle trajectories in comparison with the energy landscape is presented below.

B. Cluster 3: *N*=31

A different observation is made for the cluster with $N=31$. Figure 9 shows the trajectories of all particles in a ρ-z plot for 100 s. A shell transition with a change of the configuration is easily recognized. A particle moves from the outer shell towards the inner, resulting in a change from (4,27) to (5,26). In Fig. 10 the motion of the traveling particle is illustrated in more detail. In the beginning of the sequence, the cluster stays in the configuration (4,27) and only thermal motion of the particles is observed. However,

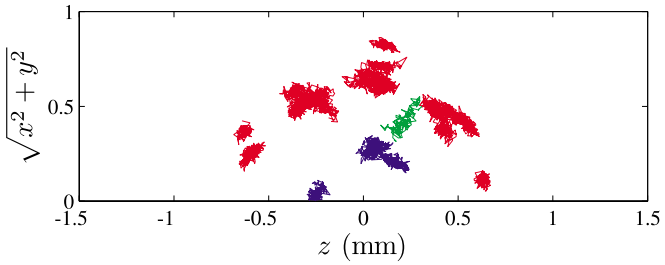

FIG. 9. (Color online) Particle trajectories in the ρ-z plane of a cluster with $N=31$. The configuration changes from (4,27) to (5,26).

after $t=430$ s a single particle starts to leave the outer shell at $r\approx 0.64$ mm. The particle moves inwards and reaches the innermost position ($r=0.34$ mm) at about $t=517$ s, where it resides for a short moment before it slowly returns to the outer shell. The positions of the other 30 particles stayed nearly constant. This transition is a very slow, gradual process. It is different from the hopping motion observed in 2D crystals occurring on the time scale of the Einstein frequency of nearest neighbor oscillations (typically of the order of a few Hertz[30]). This transition will be analyzed with respect to the energy landscape in more detail below.

C. Cluster 4 and 5: *N*=52 and *N*=91

We now will address shell transitions in larger clusters, namely, for $N=52$ and $N=91$. While the $N=31$ cluster kept a constant number of shells during the shell transition, the cluster with $N=52$ particles changes its structure between two and three shells. In a long-run experiment, this cluster was observed for 10 min. We were able to identify three different configurations during that period. The Yukawa ball remained for approximately 400 s in the (11,41) configuration. Then the configuration changes for a short time period to (10,42) and returns to (11,41). After 440 s another transition occurred where one particle moves from the outer shell

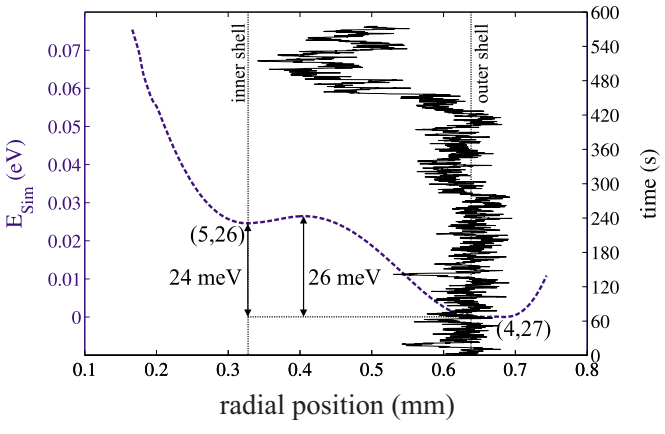

FIG. 10. (Color online) Solid curve: Radial position as a function of time for the particle traveling form the outer to the inner shell causing a configuration change from (4,27) to (5,26). Dashed curve: Energy landscape of the $N=31$ particle cluster. Here, the energy per particle E/N derived from simulation is shown for a particle traveling from the outer shell inwards. To reach the (5,26) configuration starting from (4,27) an energy barrier of 24 meV has to be overcome. Thus, the metastable configuration (5,26) is thermally accessible.

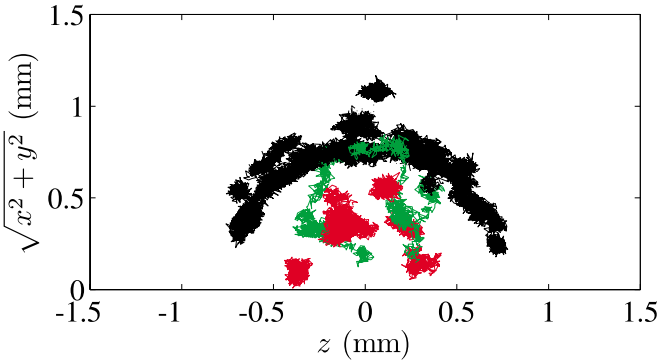

FIG. 11. (Color online) Trajectories of particles in a cluster with $N=52$ over 200 s in the ρ-z plot. Green (light gray) trajectories indicate transitions between shells, i.e., a change in the configuration occurs.

to the inner shell while another particle from the inner shell starts to travel to the center of the cluster and the configuration (1,11,40) is observed. The trajectories are shown in Fig. 11.

To analyze this in more detail, we have shown the energies of a cluster with $N=52$ particles for different selected configurations and screening strengths. The ground state configuration is (10,42) for $\kappa<0.6$.[29] For screening strengths between 0.6 and 1.4 the ground state configurations is (12,40). The configurations with a center particle (1,12,39) represents the ground state for $\kappa>1.4$. Only the experimentally observed configuration (12,40) matches a simulated ground state configuration. The other experimental configurations (11,41) and (1,11,40) are close to simulated ground states, but differ in detail. These configurations are metastable states as shown in Fig. 12.

In the experiment, the cluster shows a definite trend to higher occupation numbers of the inner shell. This can be used to deduce the screening strength κ. While in the simulation the configuration (10,42) has a low-lying energy only for small κ and is not detected for $\kappa>1.5$, the metastable configuration (1,11,40) is found only for $\kappa>0.75$. Only in a range $0.75<\kappa<1.5$ all three experimental configurations are found as low-energy states. This again supports the previous analysis on the screening strength in Sec. III.

Finally, the largest cluster with $N=91$ particles is investigated here. It consists of three shells. Indeed it has been possible to find three different configurations and self-excited transitions between them. Several traveling particles

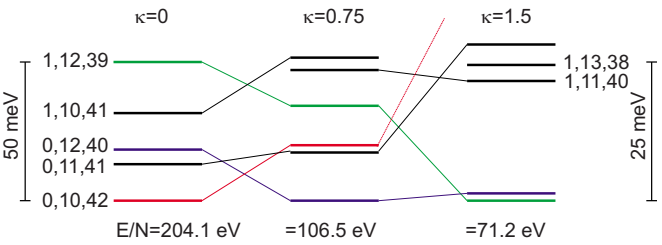

FIG. 12. (Color online) Energies of a cluster with $N=52$ particles for different selected configurations and three different values of the screening strength κ. The energies of the observed structures (11,41) and (1,11,40) are close to the ground state (12,40) for $\kappa=0.75$. The left energy scale is for $\kappa=0$, the right for $\kappa=0.75$ and 1.5.

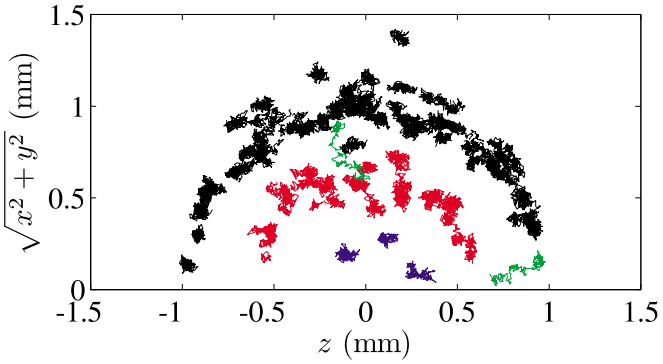

FIG. 13. (Color online) Trajectories of particles in a cluster with $N=91$ over 50 s in the ρ-z plot. Green (light gray) trajectories indicate transitions between shells, i.e., a change in the configuration occurs.

have been observed. The trajectories over 20 s are shown in the ρ-z plot in Fig. 13. The experimentally observed configurations were (3,26,62), (3,24,64), and (4,25,62).

For pure Coulomb interaction the ground state configuration is (3,22,66) (Refs. 12, 29, and 31) and the lowest-energy metastable configuration is (2,22,67). Again, we find cluster configurations that tend towards higher occupation numbers on the inner shell reflecting the shielded particle interaction.

With such long-running observations of Yukawa balls we have been able to study spontaneous transitions of particles between shells of the cluster. They also reveal the trend towards higher occupation on the inner shells.

V. DISCUSSION

From the repetition experiments and corresponding simulations two interesting findings can be concluded. First, clusters with a higher number of particles on the inner shell have an increasing probability with increasing screening and, second, the most probable configuration is not necessarily the ground state.

Both findings are illustrated in Fig. 14 which shows the simulations of the most frequently occurring configurations as well as the difference between most probable configuration and ground state as a function of the screening strength for different particle numbers. In Fig. 14(a) the occupation number of the inner shell for the most probable configuration is shown color-coded. It is seen that the most probable Yukawa ball configurations show a higher occupation number of the inner shell when the value of κ is increased. Even the formation of an additional shell is possible for a stronger shielding and particle numbers above $N=50$. In Fig. 14(b) the shaded areas indicate where the most probable state has a higher population on the inner shell compared to the ground state. Thus, there the metastable state (with higher occupation on the inner shell) is more probable than the ground state. This surprising situation is found in many cases. As an example, for $N=27$ ($\kappa=0.8$) and for $N=31$ (at $\kappa=1.1$) the above described higher probability of the metastable state is indeed observed. It is also seen that the areas of higher probability of metastable states appear close to the lines where the most probable state changes from N_1 to N_1+1 particle on the inner shell.

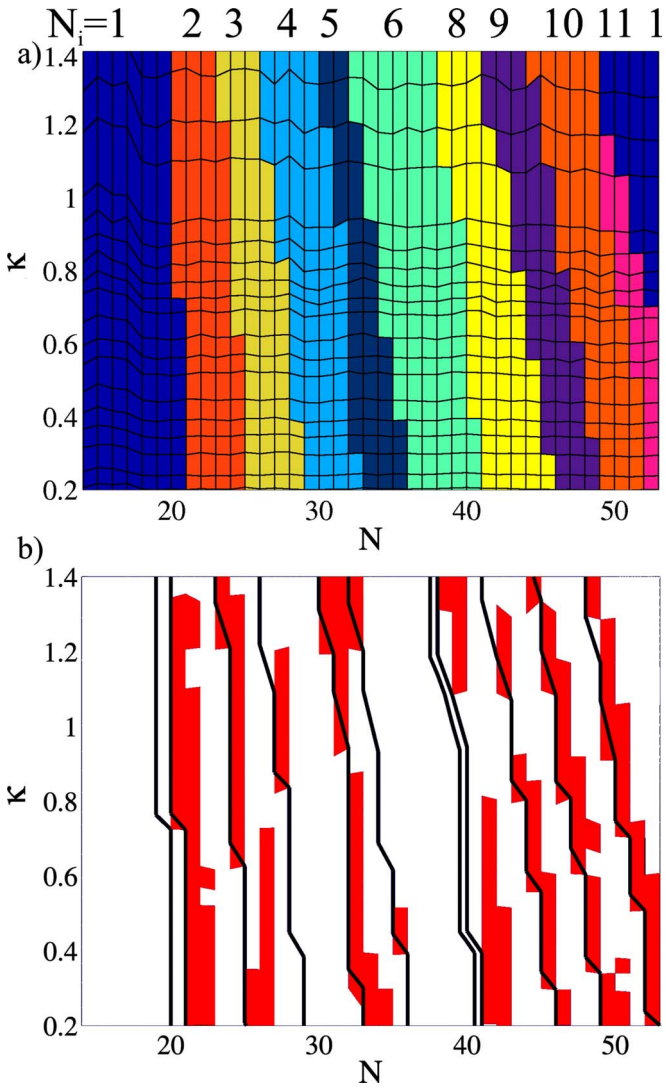

FIG. 14. (Color online) (a) Most frequently occurring configurations for different values of the screening strength. The occupation number of the inner shell is color-coded (in gray scale). For a fixed particle number N the clusters tend to show a higher occupation of the inner shells when κ is increased. (b) Difference between most probable configuration and ground state configuration. The red (grey) areas show where the metastable state has a higher probability than the ground state. The contours show where the occupation number of the inner shell changes for the most probable state as shown in (a).

This finding is not at all obvious. Indeed, it is known that in larger clusters, $N>100$, the shielded interaction affects the structure of the cluster in such a way that higher occupation numbers of inner shells and depletion of outer shell were observed.[10] In contrast, pure Coulomb systems have strictly homogeneous density.[8,27] The inhomogeneous density distribution of Yukawa balls is a consequence of the change from a global force equilibrium (due to the particular properties of the far-reaching pure Coulomb interaction) to a local balance (due to the dominance of nearest neighbors in screened interaction).[32,33] This result was obtained in a continuum model for large systems and is found to hold even for sys-

tems with only thousand particles if correlation effects are taken into account.

For small systems ($N<100$), however, the fluid approximation fails and simulations[10] indicate that the ground state shell population of small systems with screened interaction does not deviate systematically from pure Coulomb systems for experimentally accessible values of $\kappa<1.5$. However, there is no obvious reason why the principle, that short range interaction leads to overpopulation of inner shells, should not apply in small systems.

Here, we have seen that although the *energetically favored* ground state configuration does not change with $\kappa<1.5$ [e.g., the (4,27) configuration of the $N=31$ cluster] the appearance *probability* does. That means that one has a higher probability to find a metastable cluster with higher occupation number on the inner shell. Thus, *on average* the trend of a higher population of the inner shells is also observed in finite systems with $N<100$.[16] The simulated probability of different configurations for $N=27$ in Fig. 6 clearly shows a higher occupation number of the inner shell if the value of κ is increased. This goes along with the finding that the most probable configuration in many cases deviates from the ground state. To form a qualitative picture, it is instructive to compare the observed abundance of the ground and metastable states with results expected from thermodynamic considerations: In a canonical ensemble with temperature T the probabilities of a state with energy E_j is proportional to $p_j=g_j \exp(-E_j/kT)$, where g_j is the degeneracy factor, i.e., the number of states with that energy. In our case of classical distinguishable particles the number of possible realizations g of a shell configuration (N_1,N_2) simply is $(N_1+N_2)!/(N_1!N_2!)$.

Thus, the degeneracy factor of the metastable state (5,26) exceeds that of the ground state (4,27) by a factor of 27/5. This can at least partially compensate the exponential weight. For a quantitative consideration, however, a detailed analysis of the various isomeric configurations, their eigenfrequency spectra, and the nonequilibrium nature of the Yukawa balls have to be taken into account.[28] Nevertheless, a significant population of metastable states should be possible from thermodynamic considerations.

The combination of the energy levels as a function of κ [Fig. 12 and the probability map, Fig. 14(b)] forms a consistent picture: the energy of the Coulomb ground state gradually increases with an increase of κ, whereas the energy of the metastable state decreases. Near a transition in the ground state configuration the exponential weight of the energy gap can be compensated by the degeneracy factors. Then, the metastable state can become the most probable state. As a consequence, dominant metastable states are found close to transitions in the most probable configurations as indicated in Fig. 14(b).

The observation of shell transitions also lead to interesting insight to the energy landscape of Yukawa balls. For the cluster with $N=17$, we have performed MD simulations to understand the experimental observations. The curvature parameter $\alpha=2.60\times10^{-11}$ kg s^{-2} of the 3D isotropic parabolic trapping potential is chosen to match the experimental cluster size in the simulations. The screening parameter was

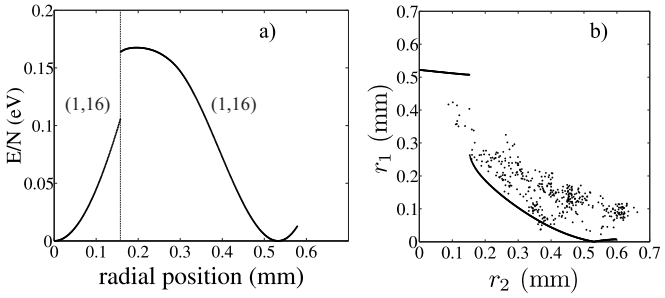

FIG. 15. (a) Energy per particle E/N of the Yukawa ball with $N=17$ when a single particle of the outer shell moves radially inward. (b) Radial position of the central particle r_1 vs the radial position of the inward moving particle r_2. Solid line: simulation; symbols: experiment.

taken as $\kappa=1$ as suggested by the afore mentioned studies of the structure and by previous investigations.[10,19] Figure 15 shows the energy of the $N=17$ particle cluster when a particle of the outer shell moves inward. Starting at a radial position of $r=0.53$ mm the cluster is in the (1,16) ground state. When with inward moving particle the cluster has reached the energy maximum ($E/N=0.17$ eV above ground state) a sudden jump in energy occurs where the central particle pops to the outer shell. Thus, it is not possible to drive a second particle into the center to achieve a (2,15) configuration. This behavior has been verified for various screening strengths in the range $\kappa=0$–3.

The experimentally observed exchange of the central and outer shell particle has also been compared to the simulation. For that purpose the radial positions of these two particles, r_1 and r_2 are plotted against each other. There, four different experimental realizations of the transition have been evaluated. Overall, the experimental particle exchange is very well reflected in the simulations. Differences occur due to slight asymmetries in the experimental confinement so that the central particle is not found at exactly $r=0$. So, the $N=17$ particle cluster is an example of a very small cluster with only a single shell (plus central particle) where shell transitions occur without configuration changes and metastable configurations are not accessible.

In the $N=31$ cluster, obviously the transition from the ground state (4,27) to the metastable state (5,26) is energetically unfavorable. Nevertheless, it has been observed in the experiments. To quantify the required energy for the transition, such a transition is calculated in a simulation. The simulated energy landscape for the transition (4,27) to (5,26) is also shown in Fig. 10. Ground and metastable states differ in energy by $E/N=24$ meV. However, to reach the metastable state an energy barrier of $E/N=26$ meV has to be overcome. These numbers indicate that the metastable state is energetically of the order of the thermal energy at room temperature.

From the experiment the energy of the traveling particle can also be estimated. With no external forces and neglected inertia (due to the slow particle motion) only friction forces act on the dust. The driving force is assumed to be the thermal Brownian motion. Thus, we have analyzed the friction energy that is dissipated by the traveling particle. The friction energy is determined from

$$\Delta E = m\beta \dot{r} \Delta r, \tag{2}$$

where the Epstein friction coefficient is $\beta = 210\ \mathrm{s}^{-1}$ for a gas pressure of 90 Pa.[34] With the shell separation $\Delta r = 3 \times 10^{-4}$ m, the particle mass of $m = 3.3 \times 10^{-14}$ kg and the transition time of $\Delta t = 87$ s the dissipated energy of the traveling particle is 45 meV which is slightly higher than that of the energy barrier and slightly above room temperature. This consistently shows that such energies are available for single particles. Thus, metastable configurations are thermally accessible in experiments at room temperature.

The numerous observed transitions in larger clusters ($N = 52$ and 91) support this interpretation. The wealth of metastable states with energies slightly above the ground state (see Fig. 12) encourage frequent configuration changes at room temperature. Since transitions of particles between different shells are a precursor of melting it should be possible to investigate phase transitions in finite clusters.[35]

VI. SUMMARY

We have presented experiments on small spherical dust clusters with special focus on shell transitions of particles to investigate the relation of structural and dynamical properties of finite dust clouds.

Metastable configurations of clusters with a fixed particle number have been repeatedly generated under identical plasma conditions. The experiments have shown that the probabilities of different metastable states depends sensitively on the range of the interaction potential of the particles. The analysis of the observed appearance probabilities from simulations and a qualitative thermodynamic argument justifies the higher probability of metastable states observed in the experiments. The comparison of the experimentally observed appearance probabilities and MD simulations allows the reliable delimitation of the screening strength κ. Thus the measurements and simulations show that the structural properties are well understood and fully consistent.

Most importantly, we succeeded in observing transitions of particles between shells. Our long-term observation of various clusters ranging from $N = 17$ to $N = 91$ particles show that shell transitions occur frequently and can be studied in detail. In a very small cluster ($N = 17$) where metastable states were not observed, nevertheless exchanges of particles without changes of the cluster configuration are found. In clusters with two shells ($N = 31$) we were able to analyze the energy landscape of shell transitions. Shell transitions can occur even from ground to metastable states when they are accessible from the particles' thermal energy. From comparison with MD simulations the energy barrier and the energy difference of different configurations were determined. Larger clusters with $N = 52$ and 91 particles show frequent transitions since many metastable states are accessible at room temperature.

Thus, here we were able to connect structural and dynamical processes in finite Yukawa systems.

ACKNOWLEDGMENTS

Financial support by the Deutsche Forschungsgemeinschaft via SFB-TR24 Grant Nos. A2, A3, A5, and A7 is gratefully acknowledged.

[1] C. C. Grimes and G. Adams, Phys. Rev. Lett. **42**, 795 (1979).
[2] R. F. Wuerker, H. Shelton, and R. V. Langmuir, J. Appl. Phys. **30**, 342 (1959).
[3] W. M. Itano, J. J. Bollinger, J. N. Tan, B. Jelenković, X.-P. Huang, and D. J. Wineland, Science **279**, 686 (1998).
[4] L. Hornekær, N. Kjærgaard, A. M. Thommesen, and M. Drewsen, Phys. Rev. Lett. **86**, 1994 (2001).
[5] M. Bonitz, P. Ludwig, H. Baumgartner, C. Henning, A. Filinov, D. Block, O. Arp, A. Piel, S. Käding, Y. Ivanov, A. Melzer, H. Fehske, and V. Filinov, Phys. Plasmas **15**, 055704 (2008).
[6] O. Arp, D. Block, A. Piel, and A. Melzer, Phys. Rev. Lett. **93**, 165004 (2004).
[7] D. Block, M. Kroll, O. Arp, A. Piel, S. Käding, Y. Ivanov, A. Melzer, C. Henning, H. Baumgartner, P. Ludwig, and M. Bonitz, Plasma Phys. Controlled Fusion **49**, B109 (2007).
[8] R. W. Hasse and V. V. Avilov, Phys. Rev. A **44**, 4506 (1991).
[9] H. Totsuji, T. Ogawa, C. Totsuji, and K. Tsuruta, Phys. Rev. E **72**, 036406 (2005).
[10] M. Bonitz, D. Block, O. Arp, V. Golubnychiy, H. Baumgartner, P. Ludwig, A. Piel, and A. Filinov, Phys. Rev. Lett. **96**, 075001 (2006).
[11] H. Baumgartner, H. Kählert, V. Golubnychiy, C. Henning, S. Käding, A. Melzer, and M. Bonitz, Contrib. Plasma Phys. **47**, 281 (2007).
[12] S. Apolinario, B. Partoens, and F. Peeters, New J. Phys. **9**, 283 (2007).
[13] A. Rahman and J. P. Schiffer, Phys. Rev. Lett. **57**, 1133 (1986).
[14] D. H. E. Dubin and T. M. O'Neil, Phys. Rev. Lett. **60**, 511 (1988).
[15] R. Rafac, J. P. Schiffer, J. S. Hangst, D. H. E. Dubin, and D. J. Wales, Proc. Natl. Acad. Sci. U.S.A. **88**, 483 (1991).
[16] D. Block, S. Käding, A. Melzer, A. Piel, H. Baumgartner, and M. Bonitz, Phys. Plasmas **15**, 040701 (2008).
[17] S. Apolinario and F. M. Peeters, Phys. Rev. E **76**, 031107 (2007).
[18] R. Quinn and J. Goree, Phys. Rev. E **61**, 3033 (2000).
[19] O. Arp, D. Block, M. Klindworth, and A. Piel, Phys. Plasmas **12**, 122102 (2005).
[20] B. M. Annaratone, T. Antonova, D. D. Goldbeck, H. M. Thomas, and G. E. Morfill, Plasma Phys. Controlled Fusion **46**, B495 (2004).
[21] M. Kroll, S. Harms, D. Block, and A. Piel, Phys. Plasmas **15**, 063703 (2008).
[22] E. Thomas, J. D. Williams, and J. Silver, Phys. Plasmas **11**, 37 (2004).
[23] S. Käding and A. Melzer, Phys. Plasmas **13**, 090701 (2006).
[24] S. Käding, Y. Ivanov, and A. Melzer, IEEE Trans. Plasma Sci. **35**, 328 (2007).
[25] Y. Ivanov and A. Melzer, Rev. Sci. Instrum. **78**, 033506 (2007).
[26] Y. Feng, J. Goree, and B. Liu, Rev. Sci. Instrum. **78**, 053704 (2007).
[27] P. Ludwig, S. Kosse, and M. Bonitz, Phys. Rev. E **71**, 046403 (2005).
[28] H. Kählert, P. Ludwig, H. Baumgartner, M. Bonitz, A. Piel, D. Block, and A. Melzer, "Probability of metastable configurations in spherical three-dimensional Yukawa crystals, Phys. Rev. E (submitted), arXiv:0805:3016.
[29] H. Baumgartner, V. Golubnychiy, D. Asmus, P. Ludwig, and M. Bonitz, "Structural transitions of finite spherical Yukawa crystals, New J. Phys. (submitted).
[30] C.-L. Chan, W.-Y. Woon, and L. I, Phys. Rev. Lett. **93**, 220602 (2004).
[31] O. Arp, D. Block, M. Bonitz, H. Fehske, V. Golubnychiy, S. Kosse, P. Ludwig, A. Melzer, and A. Piel, J. Phys.: Conf. Ser. **11**, 234 (2005).
[32] C. Henning, H. Baumgartner, A. Piel, P. Ludwig, V. Golubnychiy, M. Bonitz, and D. Block, Phys. Rev. E **74**, 056403 (2006).
[33] C. Henning, P. Ludwig, A. Filinov, A. Piel, and M. Bonitz, Phys. Rev. E **76**, 036404 (2007).
[34] P. S. Epstein, Phys. Rev. **23**, 710 (1924).
[35] J. P. Schiffer, Phys. Rev. Lett. **88**, 205003 (2002).